ACS Chemical Neuroscience

Research Article

pubs.acs.org/chemneuro

Electrochemical Investigations into Kinase-Catalyzed Transformations of Tau Protein

Meghan K. Rains,[†,‡] Sanela Martić,[†,‡,§] Daniel Freeman,[†,‡] and Heinz Bernhard Kraatz*[,†,‡]

[†]Department of Physical and Environmental Sciences, University of Toronto Scarborough, 1265 Military Trail, Toronto, ON, M1C1A4, Canada

[‡]Department of Chemistry, University of Toronto, 80 St. George St., Toronto, ON, M5S3H6 Canada

[§]Department of Chemistry, Oakland University, 2200 North Squirrel Road, Rochester, Michigan 48309, United States

Supporting Information

ABSTRACT: The formation of neurofibrillary tangles by hyperphosphorylated tau is a well-recognized hallmark of Alzheimer's disease. Resulting from malfunctioning protein kinases, hyperphosphorylated tau is unable to bind microtubules properly, causing it to self-associate and aggregate. The effects of tau phosphorylation on tau conformation and aggregation are still largely unexplored. The conformational analysis of tau and its hyperphosphorylated forms is usually performed by a variety of spectroscopic techniques, all of which require ample sample concentrations and/or volumes. Here we report on the use of surface based electrochemical techniques that allow for detection of conformational changes and orientation of tau protein as a function of tau phosphorylation by tyrosine and serine/threonine kinases. The electrochemical methods utilize 5′-γ-ferrocenyl adenosine triphosphate (Fc-ATP) derivative as a cosubstrate and tau immobilized on gold surface to probe the role of the following protein kinases: Sarcoma related kinase (Src), Abelson tyrosine kinase (Abl), tau-tubulin kinase (TTBK), proto-oncogene tyrosine protein kinase Fyn (Fyn), and glycogen synthase kinase 3-β (Gsk-3β). The single kinase and sequential kinase-catalyzed Fc-phosphorylations modulate the electrochemical signal, pointing to the dramatic changes around the Fc group in the Fc-phosphorylated tau films. The location and orientation of the Fc-group in Fc-tau film was investigated by the surface plasmon resonance based on antiferrocene antibodies. Additional surface characterization of the Fc-tau films by time-of-flight secondary ion-mass spectrometry and X-ray photoelectron spectroscopy revealed that Fc-phosphorylations influence the tau orientation and conformation on surfaces. When Fc-phosphorylations were performed in solution, the subsequently immobilized Fc-tau exhibited similar trends. This study illustrates the validity and the utility of the labeled electrochemical approach for probing the changes in protein film properties, conformation, and orientation as a function of the enzymatically catalyzed modifications.

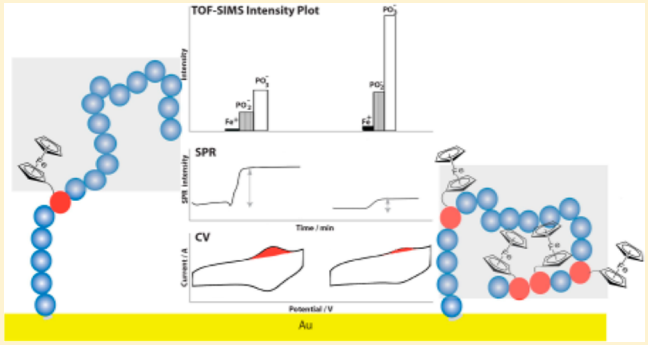

KEYWORDS: *Tau, phosphorylation, electrochemistry, ferrocene, kinase, Alzheimer's*

Tau, a microtubule associated protein, has been implicated in a number of diseases collectively termed tauopathies.[1] Among these is Alzheimer's disease, which is the leading type of dementia among the elderly.[2] The neurofibrillary tangles (NFTs) and paired helical filaments (PHFs) composed of hyperphosphorylated, aggregated tau have been implicated in neuron death and neurological degeneration.[3−6] Protein kinases, the enzymes responsible for the phosphorylation, utilize adenosine triphosphate (ATP) to transfer a negatively charged γ-phosphate group from ATP to a serine, threonine, or tyrosine residue of tau protein. This phosphate invokes a "signal-on" or "signal-off" response, regulating the tau chemical properties, conformation, and function.[7] In the native state, tau stabilizes the microtubules in the neuronal cells. Upon hyperphosphorylation, tau dissociates from the microtubules, which fall apart, and self-assembles into insoluble NFTs and PHFs.[8,9] The abnormal kinase activity is linked to Alzheimer's disease and provides an attractive target for therapy. A number of protein kinases have been found to phosphorylate tau, revealing more than 30 different phosphorylation sites in the hyperphosphorylated NFTs and PHFs.[10] The threonine/serine kinases such as Gsk-3β have been implicated in the hyperphosphorylation of tau; however, recent advances point toward phosphorylated tyrosine residues as mediators of hyperphosphorylation.[11−13] With only five tyrosine residues present in each isoform of tau, their role was initially overlooked. These residues can be systematically targeted by different tyrosine kinases to explore the role of tyrosine phosphorylation in Gsk-3β induced hyperphosphorylation. Among these kinases, Fyn, a

Received: January 19, 2013
Accepted: May 6, 2013
Published: May 6, 2013

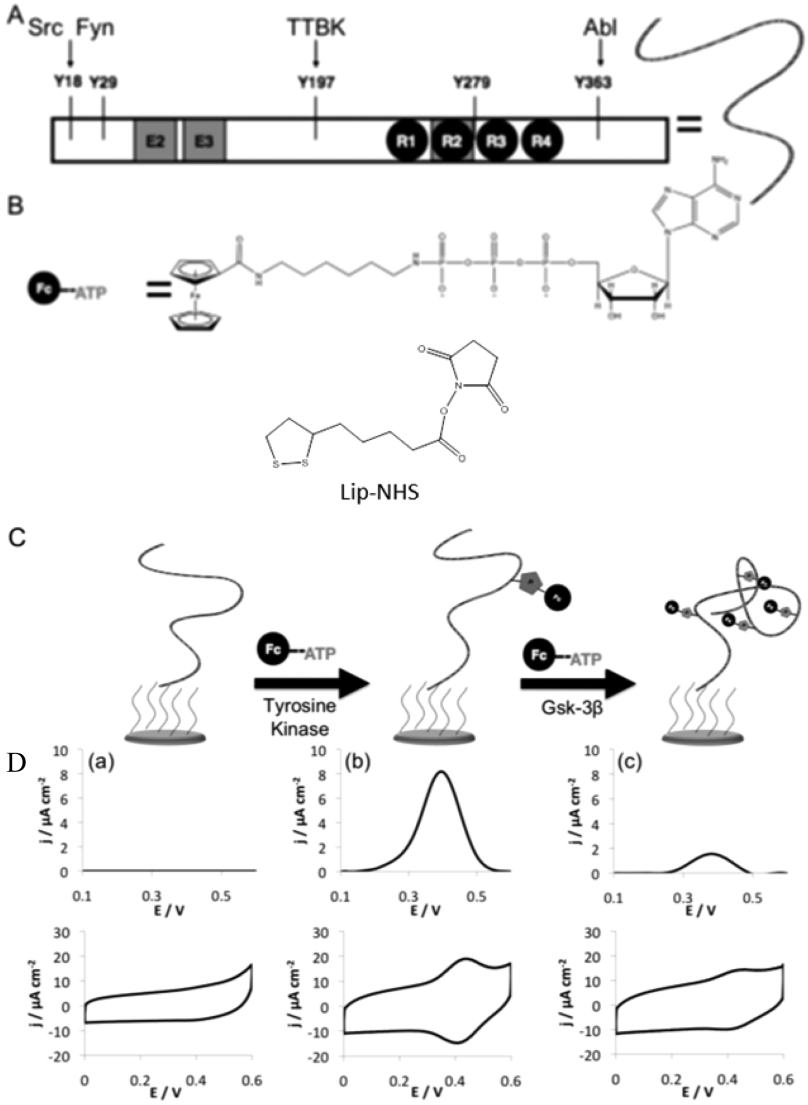

Figure 1. Overall representation of the experimental approach. (A) Schematic representation of tau410 showing the location of tyrosine residues (Y) as well as the protein kinases used to Fc-phosphorylate each. Tau contains 410 amino acid, exon 2 and 3 and microtubule binding repeats R2-R4. (B) Structures of Fc-ATP cosubstrate used throughout experimental approach for Fc-phosphorylation and the Lip-NHS. (C) Schematic representation of the immobilized tau, the single tyrosine kinase Fc-phosphorylation followed by the sequential GSK-3β Fc-phosphorylation. (D) The square-wave voltammograms (SWVs) (top) and cyclic voltammograms (CVs) (bottom) of the surface-bound tau (a), Fc-tau phosphorylated by a single tyrosine kinase (b) followed by the sequential GSK-3β Fc-phosphorylation (c). SWVs were background subtracted for clarity, and CVs illustrate actual measurements. An increase in current density was observed when a single tyrosine Fc-phosphorylation was carried out (b), and a dramatic decrease was observed upon sequential Fc-phosphorylation (c).

member of the Src family, has been shown to phosphorylate tau at tyrosine 18.[13,14] Implicated in neurodegeneration pathways initiated by β-amyloid, Fyn has been widely studied, finding that both Fyn-negative cells and tau-negative cells are protected from β-amyloid induced neurotoxicity.[15,16] A related kinase, Src, has also been shown to phosphorylate tau at tyrosine 18, but it has received less attention than Fyn. Though the exact phosphorylation sites of tau have been vastly explored, the effects of phosphorylation, hyperphosphorylation, and sequential phosphorylation of tau on its conformation, folding, and aggregation are less understood. The conventional methods for the detection of the site-specific phosphorylations of tau include the Western blotting and mass spectrometry.[17,18] The tau aggregation is typically explored by electron microscopy and fluorescence spectroscopy,[19,20] while the conformational analysis of tau forms have been investigated by UV−vis, IR, and circular dichroism spectroscopies.[21] Each technique targets a specific event: the phosphorylation levels/sites of tau, the consequential effects of hyperphosphorylation on tau conformation and aggregation, or the nature of aggregates formed.

In this paper, we report an electrochemical surface-based approach for monitoring the effects of tau ferrocene (Fc)-phosphorylation on tau410 (Figure 1A) conformation. This research utilizes a redox active cosubstrate to investigate a single kinase and sequential kinase Fc-phosphorylations of immobilized tau protein. Unlike ATP, which is a redox-silent cosubstrate, 5′-γ-ferrocenyl adenosine triphosphate (Fc-ATP, Figure 1B) produces the electrochemical signal when incorporated into surface-bound peptide or protein.[22,23] In addition, Fc-phosphorylation of immobilized tau protein, by a single protein kinase, was recently demonstrated electrochemically.[24] However, these electrochemical studies were limited to

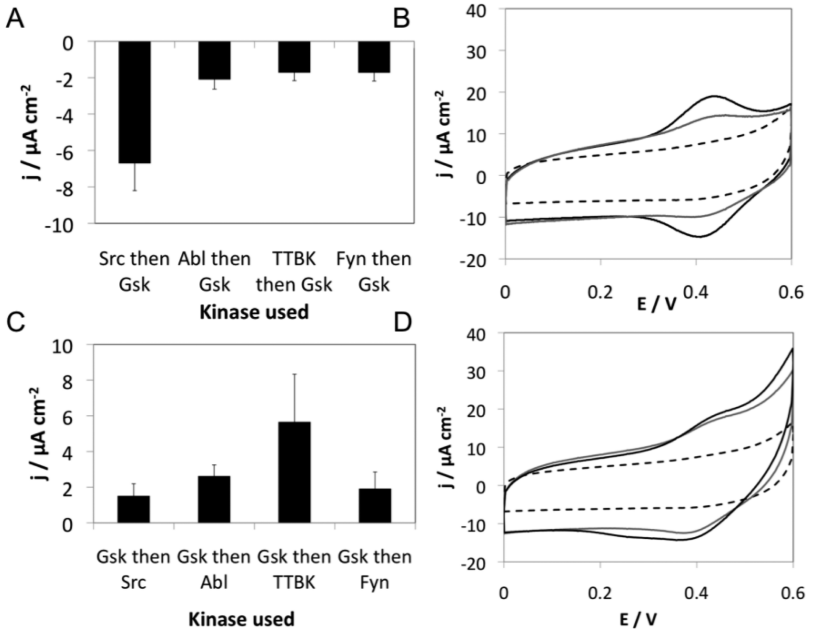

Figure 2. Surface electrochemical results of the Fc-phosphorylations carried out on surfaces. The single kinase and sequential kinase Fc-phosphorylations were carried out on surfaces, and the electrochemical response measured. (A) Change in current density observed in background-subtracted SWVs when tau was initially Fc-phosphorylated with a tyrosine kinase followed by Gsk-3β. (B) Representative CVs obtained for just tau (dashed black), Fc-phosphorylation by a tyrosine kinase (solid black), and sequential Fc-phosphorylation by Gsk-3β (solid gray). (C) Change in current density observed in background-subtracted SWVs when tau was initially Fc-phosphorylated with Gsk-3β followed by a tyrosine kinase. (D) Representative CVs obtained for tau (dashed black), Fc-phosphorylation by Gsk-3β (solid gray), and sequential Fc-phosphorylation by a tyrosine kinase (solid black). All measurements were recorded in 2 M sodium perchlorate buffer (pH of 6.1) vs Ag/AgCl, Pt as auxiliary electrode, and tau-modified gold electrode as working electrode. All measurements were recorded from the open circuit potential in the negative direction at a scan rate of 100 mV s^{-1}. Error bars represent standard error of triplicate measurements.

the Fc-phosphorylations by a single kinase and did not report on the tau protein film properties, such as conformation, and orientation. In the proposed approach, the Fc-ATP serves as a handle for probing two biochemical events in a single electrochemical platform: (1) the Fc-phosphorylation of tau by multiple kinases (single and sequential phosphorylations) and (2) the changes in the Fc-tau film properties due to the Fc-tau conformational changes and folding. In this context, Fc-group is introduced at the phosphorylation site and serves as a signaling probe and a reporter of the conformational changes of tau protein, induced by the kinase-catalyzed phosphorylations. Due to the redox-activity of the immobilized Fc-tau on gold surfaces, the current response was monitored and served as the indirect measure of the changes associated with Fc-tau films. We have investigated how Fc-phosphorylation type and sequence affect the conformation and orientation of the surface-bound Fc-tau protein. This study explores and compares tau film orientation, conformation, and properties on gold surfaces as a function of the Fc-phosphorylations in single and sequential Fc-phosphorylation formats. The complementary solution Fc-phosphorylations studies were used to gain understanding about the role of the surface immobilization on tau phosphorylation and conformation. The Fc-tau protein films were characterized using surface plasmon resonance (SPR), time-of-flight secondary ion mass spectrometry (TOF-SIMS), and X-ray photoelectron spectroscopy (XPS). Our results imply that the type and sequence of single and sequential Fc-phosphorylations play important roles in the Fc-tau protein orientation and conformation.

RESULTS AND DISCUSSION

Prior to the electrochemical studies, the clean gold surface was immobilized with the lipoic acid *N*-succinimide active ester, according to the literature protocol.[25] The first electrochemical sensor of this kind, previously reported by Kerman et al.,[25] was based on the immobilization of a peptide sequence on the surface of a gold electrode via covalently bound lipoic acid *N*-succinimide active ester, and subsequent Fc-phosphorylation of the peptide. Here, we utilize the same approach to immobilize tau-410 via N-terminus or available lysine residues (Figure 1C). The human tau-410 illustrated in Figure 1A contains a total of five tyrosine residues, located at positions 18, 29, 197, 279, and 363. The kinase-catalyzed Fc-phosphorylations were carried out in two different ways: a single kinase Fc-phosphorylation or a sequential kinase Fc-phosphorylation.

To carry out the single kinase Fc-phosphorylation (Figure 1C), we have chosen a number of tyrosine protein kinases: Sarcoma-related (Src), Proto-oncogene tyrosine protein kinase Fyn (Fyn), Tau-tubulin kinase (TTBK), and Abelson tyrosine kinase (Abl). The targeted Fc-phosphorylation of tyrosine residues was carried out at the *N*-terminus, the proline-rich region proximal to the microtubule binding domain, and *C*-terminus of tau. We have utilized electrochemical surface-based techniques, cyclic voltammetry (CV) and square-wave voltammetry (SWV), to monitor the single and sequential Fc-phosphorylations, and their effects on Fc-tau film properties as illustrated in Figure 1D. Prior to Fc-phosphorylations, no electrochemical signal was observed for tau films on gold (a) (Figure 1D). The single kinase-catalyzed Fc-phosphorylation was carried out in the presence of Fc-ATP and an appropriate tyrosine kinase, and subsequently monitored by CV (Figure 1D

(bottom)) and SWV (Figure 1D (top)). In general, Fc-tau films (b) prepared by a single kinase phosphorylation were characterized by an oxidation potential at ~410 ± 10 mV vs Ag/AgCl (Figure 1D). The variation in the current density was observed for a series of tyrosine kinases (Src, Fyn, Abl, and TTBK), and may be attributed to their lower kinase activities, pH dependency, and the location of the phosphorylation site.[26,27]

After initial tyrosine Fc-phosphorylation of tau, the sequential Fc-phosphorylation was mimicked utilizing Gsk-3β to phosphorylate a number of serine/threonine residues (Figure 1C). It was initially hypothesized that the electron density would rise sharply due to the increased number of serine/threonine residues available for Fc-phosphorylation by GSK-3β.[2,10] The typical electrochemical results of this study are illustrated in Figure 1D, showing a decrease in the current density in the SWVs and CVs upon sequential Fc-phosphorylation by GSK-3β (c). From the surface electrochemical measurements, we noted a general current density decrease instead of increase for all of the sequential Fc-phosphorylations (Figure 2A). The greatest reduction in current density was observed after the Src phosphorylated tau was Fc-phosphorylated with Gsk-3β, decreasing the current density from 8.49 ± 1.20 μA cm^{-2} to 0.81 ± 0.28 μA cm^{-2} (Figure 2A). This dramatic decrease was clearly observed in CV, Figure 2B. Electrochemical parameters determined for different Fc-tau films show similar trends for different tyrosine kinases and sequential Fc-phosphorylations.

A dramatic decrease in the electrochemical signal upon sequential Fc-phosphorylation may be due to the loss of the Fc group, the changes in distance between the Fc group and electrode, and/or the changes in the desolvating and chemical environment around Fc group in the Fc-tau films. The additional washings of the electrodes did not produce lower electrochemical signal, pointing to the stability of the Fc-tau films and no loss of the Fc-group.

The reverse sequential Fc-phosphorylation was also performed to further study the effects of tyrosine phosphorylation and the importance of the phosphorylation sequence. To adequately probe this challenging system, we chose to reverse the order of Fc-phosphorylation events by performing initially the Gsk-3β Fc-phosphorylation followed by a sequential tyrosine Fc-phosphorylation. The reverse sequential electrochemical results are illustrated in Figure 2C and D, and show an overall trend of increasing current density upon sequential Fc-phosphorylation. The positive change in the current density values ranged from 1.52 to 5.66 μA cm^{-2} depending on the tyrosine kinases used. The greatest increase in the current density was obtained for the Gsk-3β/TTBK pair, while the smallest increase was observed for the Gsk-3β/Src kinases. The other two systems (Gsk-3β/Abl and Gsk-3β/Fyn) produced similar increases to the Gsk-3β/Src pair. The electrochemical data indicate that the relative trends in the current density are highly dependent on the sequence of the single and sequential Fc-phosphorylations. For example, the single tyrosine kinase Fc-phosphorylation, followed by the Gsk-3β kinase sequential Fc-phosphorylation, induced a decrease in the current density. But by reversing the order of Fc-phosphorylation, the trend in the electrochemical signal was also inverted. Hence, the electrochemical signal is related to the properties of the Fc-tau protein films, and not due to the loss of the Fc group. The electrochemical investigations show that the sequential Fc-phosphorylations are feasible, and a negligible amount of surface bound material is lost between washing and incubation steps. The chemical immobilization of tau may affect the Fc-phosphorylation, Fc-tau film properties, and the electrochemical signal upon single kinase and sequential kinase Fc-phosphorylations. Previous research has shown that immobilized proteins are able to retain their function,[28,29] despite the "unnatural" conformation of the proteins on surfaces. By immobilizing a protein on an electrode surface, a secondary structure is superimposed, which may also influence protein conformation.[30−32] When tau is immobilized on the gold electrode, it may be undergoing a number of different interactions, not representative of the native state. For this reason, we chose to investigate the effects of carrying out the Fc-phosphorylations in solution prior to surface immobilization, as illustrated in Figure 3. By allowing tau to adopt its most stable conformation in solution and at physiological pH, nonnative interactions are minimized and thus provide a more realistic scenario to in vivo conditions. After the single kinase (Figure 3A) or sequential kinase Fc-phosphorylations (Figure 3B) of tau in solution, in a manner similar to that previously reported, Fc-tau was subsequently immobilized on gold surface, as shown in Figure 3, and its electrochemical properties evaluated as mentioned before.

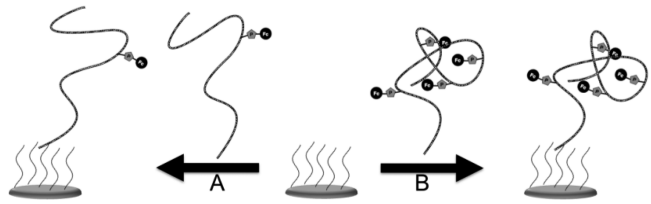

Figure 3. Immobilization of the solution Fc-phosphorylated tau. Solution-based phosphorylation allows tau to adopt most stable conformation while undergoing modification and subsequent conformational changes. (A) Immobilization of tau Fc-phosphorylated by a tyrosine kinase. (B) Immobilization of tau Fc-phosphorylated at multiple residues after sequential phosphorylation.

This assay was performed in both the forward and reverse sequential directions, giving valuable information regarding the role of surface confinement on tau orientation and conformation. The single kinase and sequential kinase Fc-phosphorylations of tau in solution ensure that the native form of tau is retained. Next, Fc-tau was immobilized on gold via Lip-NHS as previously mentioned (Figure 3). This is the first example of immobilizing an in situ Fc-phosphorylated protein. If the immobilization of the Fc-tau on the surface was successful, then significant electrochemical signal is expected. The results of this study are displayed in Figure 4A, showing a decrease in current density when a single tyrosine Fc-phosphorylation is followed by a sequential GSK-3β Fc-phosphorylation. CV also shows the dramatic decrease in the current density (Figure 4B). When the Fc-phosphorylation was performed in the reverse manner (Gsk-3β Fc-phosphorylation followed by the sequential tyrosine Fc-phosphorylation), then the current density increased (Figure 4C,D). Importantly, the electrochemical trends parallel those obtained from the surface-based Fc-phosphorylations, indicating that tau's native form and native interactions are maintained on surfaces, further strengthening the validity of the surface electrochemical approach based on Fc-ATP for probing enzymatic events such as protein transformations. We propose that the introduction of the Fc-phosphate groups creates the charge

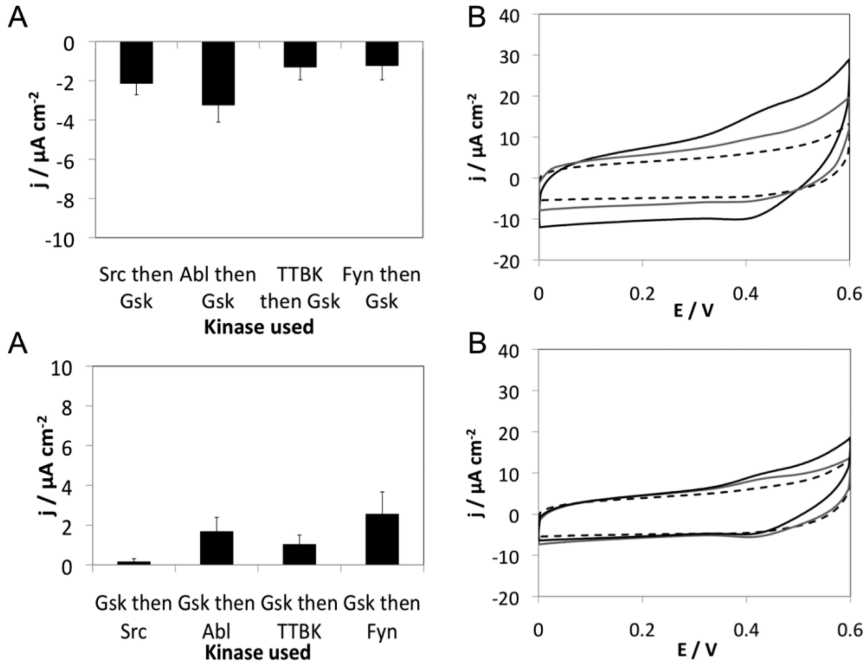

Figure 4. Surface electrochemical results of the Fc-phosphorylations carried out in solution. The single kinase and sequential kinase Fc-phosphorylations were carried out in solution. The Fc-tau was then immobilized and the electrochemical response measured. (A) Change in current density for tau initially Fc-phosphorylated by a tyrosine kinase then sequentially Fc-phosphorylated by Gsk-3β. (B) Representative CVs obtained for tau (dashed black), Fc-phosphorylated tau by a tyrosine kinase (solid black), and sequentially Fc-phosphorylated tau by Gsk-3β (solid gray). (C) Change in current density for tau initially Fc-phosphorylated by Gsk-3β then sequentially Fc-phosphorylated by a tyrosine kinase. (D) Representative CVs obtained for tau (dashed black), Fc-phosphorylated tau by Gsk-3β (solid black), and sequentially Fc-phosphorylated tau by tyrosine kinase (solid gray). All measurements were recorded in 2 M sodium perchlorate buffer (pH of 6.1) vs Ag/AgCl, Pt auxiliary electrode, tau-modified gold working electrode. All measurements were recorded from the open circuit potential in the negative direction at a scan rate of 100 mV s^{-1}. Error bars represent standard error of triplicate measurements.

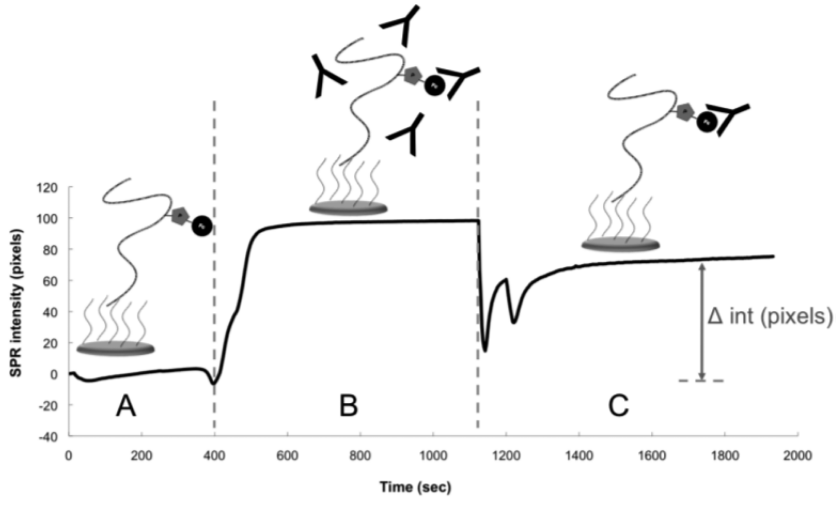

Figure 5. SPR profile of the anti-Fc antibody binding to the single kinase Fc-phosphorylated tau films. (A) The surface was rinsed with TBST buffer and then allowed to stabilize. (B) A solution of anti-Fc antibody in TBST was introduced over the Fc-tau film. A rise in intensity was observed due to the anti-Fc antibodies binding to Fc groups in Fc-tau film. (C) TBST buffer was introduced to remove nonspecifically bound anti-Fc antibodies, yielding a change in SPR intensity (Δint (pixels)).

imbalance and forces the Fc-tau to adapt by undergoing conformational changes and folding on surfaces. Differences in the electrostatic interactions and structural changes induced by the Fc-phosphorylations potentially affect the distance between the Fc group and the electrode, and the environment around the Fc group in the film, and modulate the electrochemical signal.

To explore the Fc-tau film properties, and the orientation of the Fc-group in the Fc-films, additional surface-based characterization studies were performed. We chose to investigate a representative single kinase and sequential kinase Fc-phosphorylations using a tyrosine kinase, Src, and Gsk-3β, by surface plasmon resonance (SPR), time-of-flight secondary ion mass spectrometry (TOF-SIMS), and X-ray photoelectron spectroscopy (XPS). These techniques will reveal valuable

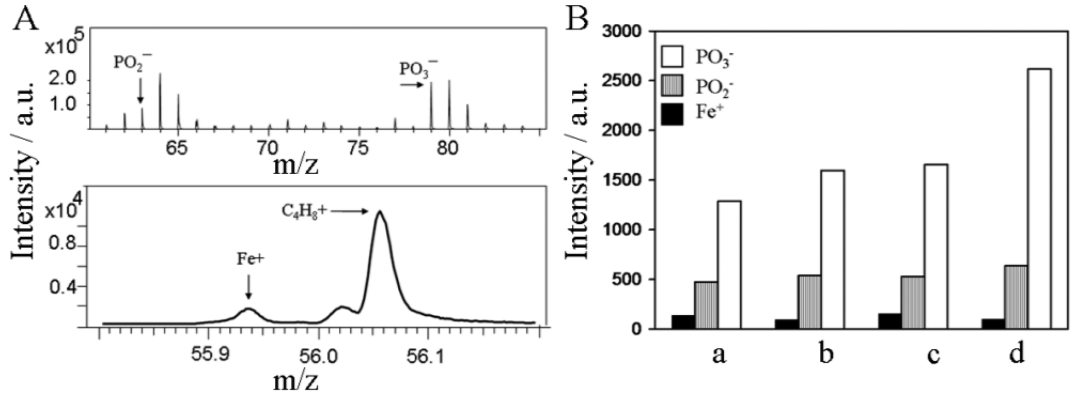

Figure 6. TOF-SIMS analysis of the Fc-tau films prepared by the single kinase or sequential kinase Fc-phosphorylations. (A) Negative ion (top) and positive ion (bottom) mode TOF-SIMS spectra of Fc-tau films prepared by a single kinase Fc-phosphorylations on surface. (B) Plot of PO_3^-, PO_2^-, and Fe^+ ion intensities as a function of the Fc-tau film type following: (a) Src, (b) Src then Gsk-3β, (c) Gsk-3β, and (d) Gsk-3β then Src Fc-phosphorylations on surfaces.

information regarding the Fc-group in protein film and the orientation of the Fc-tau film on surfaces. The surface immobilization of tau on gold substrates, for the surface studies, was performed in a similar manner to the electrochemical experiments. Fc-phosphorylations of the surface bound tau was carried out under the identical conditions as previously indicated for electrochemical measurements. Four representative Fc-tau films were prepared in the presence of Src, Src then GSK-3β, GSK-3β, and GSK-3β then Src protein kinases.

In an SPR format, the Fc-tau films were exposed to the antiferrocene (anti-Fc) antibodies. We recently showed that anti-Fc antibodies are able to bind Fc-phosphorylated peptides and Fc-phosphorylated proteins.[23] The antigen−antibody interaction was used to probe the extent of Fc-phosphorylation and the availability of the Fc-group in Fc-tau films. After the SPR chip was appropriately blocked for the nonspecific adsorption, the SPR was recorded as a function of the flow-in solution as illustrated in Figure 5. Initially, the TBST buffer was flown in over the Fc-tau film (Figure 5A). After a baseline was established, the anti-Fc antibody was added and allowed to equilibrate (Figure 5B). Subsequently the SPR chip was rinsed with TBST buffer to remove excess anti-Fc antibody, causing a change in the SPR intensity (Figure 5C). After the final period of buffer rinsing, the change in SPR intensity (Δint (pixels)) was calculated. As illustrated in Figure 5, the anti-Fc antibody binding to the Fc-tau phosphorylated by a single tyrosine kinase showed an increase of 63.9 $\pm$ 5.0 pixels. By contrast, negligible SPR signal was observed for a sequential Fc-phosphorylation with Gsk-3β, agreeing well with the electrochemical data. When the reverse sequential phosphorylation was performed with Gsk-3β negligible SPR response was obtained. However, a small increase in Δint of ~0.68 $\pm$ 0.07 pixels was recorded when sequentially Fc-phosphorylated with a tyrosine kinase. This trend parallels the electrochemical data. The antibody−antigen binding kinetics were calculated by fitting the experimental SPR data to a 1:1 binding model. The average k_{on} rate constants were determined to be $16 \times 10^{-3} \pm 0.01$, $4.0 \times 10^{-3} \pm 0.0007$, $8.0 \times 10^{-3} \pm 0.001$, and $10 \times 10^{-3} \pm 0.0006$ s^{-1} for Src, Src then Gsk-3β, Gsk-3β, and Gsk-3β then Src Fc-tau films, respectively. The SPR results indicate that the availability of the Fc-group to anti-Fc antibodies in Fc-tau films is highly dependent on the type and sequence of the single kinase or sequential kinase Fc-phosphorylations. When the Fc-group is accessible to the anti-Fc antibodies, then the SPR signal is observed. However, when Fc-group is buried in the Fc-tau film, then it is unable to interact with the anti-Fc antibodies, giving rise to a low SPR signal. The trend observed for changes in the SPR intensities parallels the electrochemical trends and confirm the notion that the Fc-phosphorylations induce the electrostatic and conformational changes within the Fc-tau protein films.

The electrostatic and conformational changes and protein folding on surfaces may be caused by Fc-phosphorylations, and may burry the Fc group, leading to the decrease in current density, and reduced anti-Fc antibody binding. The low binding of an antibody to an antigen was recently attributed to the steric hindrance, surface charge, and improper orientation of either partner.[33]

Next, the chemical composition of the Fc-tau films on surfaces was investigated by TOF-SIMS.[34,35] The amino acid content determination and the elucidation of the conformation and orientation of albumin, myoglobin, and fibrinogen proteins were previously achieved by this method.[36,37] In addition, TOF-SIMS analysis of the Fc-phosphorylated peptide films on gold surfaces was also reported.[38] Following the successful single kinase or sequential kinase Fc-phosphorylations of immobilized tau, TOF-SIMS spectra of the Fc-films were acquired. The Fc-tau films prepared under different experimental conditions were analyzed for Fe^+, PO_2^-, and PO_3^- ion contents which are indicative of the Fc-phosphorylations. We hypothesize that the greater degree of the Fc-phosphorylation (upon sequential Fc-phosphorylations) will result in the higher ion counts, assuming the identical protein orientation on surfaces. Figure 6A shows a typical negative ion and positive ion mode TOF-SIMS spectra for the Fc-tau films phosphorylated by a single protein kinase. The ions found at 55.9, 62.9, and 78.9 m/z correspond to the Fe^+, PO_2^-, and PO_3^- species, respectively, and indicate successful Fc-phosphorylation of a surface-bound tau. Similar TOF-SIMS profiles were observed for all single kinase and sequential kinase Fc-phosphorylations. In addition, the Fc-tau films prepared by the surface-assisted or solution Fc-phosphorylations were characterized by the presence of all three indicative ions.

In general, the ion content in Fc-tau films, following the sequential Fc-phosphorylations, is greater than that after the single kinase Fc-phosphorylation (Figure 6B). However, the relative intensities of ion peaks differ depending on the type

dx.doi.org/10.1021/cn400021d | ACS Chem. Neurosci. 2013, 4, 1194−1203

and sequence of the Fc-phosphorylations. From the relative intensities in Figure 6B, it is evident that GSK-3β/Src Fc-phosphorylations (d) gave rise to the highest ion intensities. The variations in the ion content may be due to the amount of the Fc groups incorporated into the Fc-tau films or the orientation of Fc-tau films, since the sampling depth of TOF-SIMS is ~1−1.5 nm, which is lower than the typical protein dimension (4−10 nm).[34] The typical sampling depth for molecular fragments is ~2 nm, but larger depth is expected for atomic species such as Fe^+. The overall TOF-SIMS ion intensities may reflect only the outer surface of the Fc-tau film. Hence, the conformation of the Fc-tau may vary with the Fc-phosphorylation type and sequence. At present, TOF-SIMS analysis reflects the sampling of the specific Fc-tau regions and gives an incomplete picture of the Fc-phosphate distribution. However, TOF-SIMS may be sensitive to the Fc-tau conformation and orientation on surfaces. For this purpose, the positive ion intensities associated with the amino acid fragments were analyzed. This type of amino acid analysis has been previously applied to the TOF-SIMS data treatment for several surface bound proteins.[34,35] All amino acids located at the top surface of the protein film are exposed and may contribute to the ion fragments during TOF-SIMS measurements. All Fc-tau films were characterized by relatively low ion intensities associated with following amino acid fragments: Leu/Ile (86 m/z), Tyr (107 and 136 m/z), Arg (110 m/z), Phe (120 m/z), and Trp (131 m/z), presumably due to the low abundance of these residues in tau protein. The highest ion intensity was observed for Pro (68 and 70 m/z) fragments in the Fc-tau films prepared by a single kinase or sequential kinase Fc-phosphorylation. Pro residues are typically found in the middle of the tau sequence called Pro-rich region or in the microtubule-binding domain. This suggests that the overall Fc-tau protein may assume a closed conformation. However, the peak at m/z = 70 was also previously assigned to a number of overlapping amino acids, such as Pro, Arg, Leu, and Lys, and may represent the heterogeneity of the surface conformation and orientation of the Fc-tau.[39] The single tyrosine Fc-phosphorylation resulted in the highest ion intensities for Ser, Pro, and Thr, which decreased upon sequential kinase Fc-phosphorylation. Most Ser and Pro amino acids in tau may be found in the middle or at the end of the C-domain. Hence, the relative ion intensities difference between the single kinase and sequential kinase Fc-phosphorylations suggests largely different Fc-tau orientations. Importantly yet, the reverse order in amino acid fragment intensities was observed for initial Fc-phosphorylations with Gsk-3β followed by the sequential tyrosine Fc-phosphorylations. This also points to the effective change in the Fc-tau conformation as a result of different Fc-phosphorylation. Interestingly, slight differences were observed for Ser (60 m/z), Pro (70 m/z), Val (72 m/z), and Thr (74 m/z) residues for the Fc-films prepared by surface-assisted and solution Fc-phosphorylations. These differences may point to the alternative orientations of the Fc-tau films on surfaces, and incomplete immobilization. By comparing the TOF-SIMS data with the SPR analysis, we may conclude that the Fc-group is not always located at the outermost surface of the Fc-tau film, and its location is dictated by the Fc-phosphorylation type and sequence.

In order to probe the composition of the Fc-tau films as a function of a single kinase or sequential kinase Fc-phosphorylation, XPS analysis was carried out on four representative Fc-tau films prepared in the presence of (a) Src, (b) Src/GSK-3β, (c) GSK-3β, and (d) GSK-3β/Src. Selected XPS atomic intensities are provided in Table S2 in the Supporting Information. All protein films were characterized by the strong S 2p core level binding energy and two doublets (associated with the bound and unbound forms of sulfur).[40,41] The relative ratio of the two peaks within each doublet was 2.000 ± 0.003 for all films which matches well the theoretical 2:1 ratio due to the spin−orbit coupling of the 2p electrons. In addition, the doublet-to-doublet area ratio for bound and unbound sulfur was 4.64 ± 0.46, and suggested no loss of tau protein from surfaces even after sequential phosphorylations. Comparison of the XPS spectra of the bare gold with those with immobilized tau indicates the reduction in the Au 4f peak at 79.95 eV, from 64% to ~47% due to tau binding. From the film thickness for the Lip-NHS on gold,[23] and the specific Au 4f intensities, the Fc-tau film thickness was estimated to be in the 1.3−1.4 nm range using the average polymer electron attenuation length (EAL).[42] In addition, Fc-tau films are characterized by a significant N 1s content at 400 eV which was absent from the clean bare gold control.[43] All tau films exhibited similar XPS elemental composition, and no significant change in the composition was observed after sequential kinase Fc-phosphorylations indicating no loss of protein from the surface following the enzymatic transformations.

The results of the present study suggest that our electrochemical method is a viable tool for studying the reorientation and conformational changes of tau protein films upon Fc-phosphorylation. A larger electrochemical signal was observed for tau film prepared with a single Tyr Fc-phosphorylation compared to a tau film prepared with Gsk-3β hyperphosphorylation (Figure 7). In addition, tau films prepared by sequential Src then Gsk-3β or Gsk-3β then Src Fc-phosphorylations do not have similar electrochemical profiles, further pointing to the importance of the Fc-phosphorylated protein conformation and reorientation and their effect on the

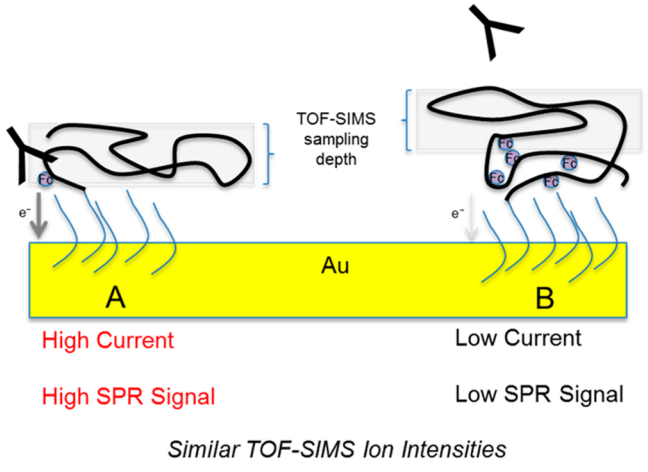

Figure 7. Schematic illustration of immobilized tau films Fc-phosphorylated by (A) Src and (B) Src then Gsk-3β protein kinases. The high current was observed for tau film with a single Fc-phosphorylated site. The low current is due to the change in the location of Fc-group, the distance of the Fc-group from the electrode, and the environment around the Fc-group. The antiferrocene antibodies bind to the accessible Fc-group in the tau film with a single Fc-phosphorylated site (A), but not to the inaccessible Fc-groups in (B). The TOF-SIMS sampling depth is shown and remains constant throughout the measurement.

analytical signal. The modulation in the current reflects the changes in the distance of Fc-group from the electrode, and/or environment around the Fc-group in the tau film due to the conformational changes and reorientation induced by the Fc-phosphorylations. This behavior is depicted in Figure 7. SPR data further point to the effects of Fc-phosphorylations on the protein films. Antiferrocene antibodies bind Fc-tau films when Fc-group is exposed, but fail to interact with Fc-tau films when Fc-groups are buried and inaccessible (Figure 7). The SPR data revealed that the Fc-phosphorylated tau films may have inaccessible Fc-groups despite the high phosphorylation levels. The constant TOF-SIMS sampling depth further suggests that the level and sequence of Fc-phosphorylation affect the protein film conformation and reorientation. Following the single or sequential Fc-phosphorylation of tau films, similar ion intensities were observed in the TOF-SIMS study (Figure 7). This is likely in the event that the Fc-tau films adopt a variety of conformations provided the identical sampling depth (2−6 nm).

The combined electrochemical, SPR, and TOF-SIMS analyses support that the level and the order of Fc-phosphorylations greatly affect the reorientation and conformation of Fc-tau films. These findings point to the significant early on-set changes of tau much before the formation of paired helical fillaments or neurofibrillary tangles.

■ CONCLUSIONS

In summary, we have shown the utility of a surface-based electrochemical approach for investigation of the protein film properties using the Fc-phosphorylated tau. The change in the electrochemical signal corresponded to a change in the properties of the protein films due to the kinase-catalyzed transformations. Fc-phosphorylations introduced the electrostatic charges in tau, and triggered the changes in the Fc-tau film orientation and conformation on surfaces. The effects of the Fc-phosphorylations on the electrochemical signal were similar for solution and surface kinase-catalyzed transformations, pointing to the validity of the surface-based electrochemical platform for investigations of protein film modifications and protein structural changes. This work also highlights the value of a surface based electrochemical approach to monitor early changes in the structure and conformation of protein targets related to neurodegenerative diseases.

■ METHODS

Sarcoma related kinase (Src), tau-tubulin kinase (TTBK), proto-oncogene tyrosine protein kinase Fyn (Fyn), glycogen synthase kinase 3 β (Gsk-3β), and Tau 410 were purchased from SignalChem (Richmond, BC). Abelson tyrosine kinase (Abl) was purchased from New England Biolabs (Pickering, ON). All kinases and tau protein were used without further modification. Fc- ATP was synthesized as previously reported.[44] 3-(*N*-Morpholino)propanesulfonic acid (MOPS), β-glycerophosphate, and tris(hydroxymethyl)aminomethane hydrochloride (Tris-HCl) were purchased from Sigma Aldrich and used as provided. Magnesium chloride ($MgCl_2$) was purchased from Caledon, and manganese chloride ($MnCl_2$), ethylenediaminetetraacetic acid (EDTA), and ethyleneglycoltetraacetic acid (EGTA) were supplied from BioBasic Inc. All electrochemical measurements were performed using a CHI 650C potentiostat and 0.02 cm^2 microcrystalline gold disk electrodes purchased from CHInstruments (Austin, TX). All buffers were prepared using ultrapure water (18.3 MΩ cm) using a Milli-Q system (Millipore, MA). Ethanol was freshly distilled prior to use. Serum enriched with polyclonal rabbit antiferrocene antibodies were produced at YenZym Antibodies, LLC (San Francisco, CA) against the monosubstituted ferrocene-amide-alkylamine. Antiferrocene antibodies were used without further purification at 1:1000 dilution in 0.1% bovine serum albumin (BSA) in Tris buffer saline Tween-20 (TBST).

Kinase Buffers. Kinase buffers were prepared according to manufacturer's specifications for each kinase. Gsk-3β and TTBK buffer contains 25 mM MOPS (pH 7.2), 12.5 mM β-glycerophosphate, 25 mM $MgCl_2$, 5 mM EGTA, and 2 mM EDTA. Src buffer contains 5 mM MOPS (pH 7.5), 2.5 mM β-glycerophosphate, 4 mM $MgCl_2$, 2.5 mM $MnCl_2$, 1 mM EGTA, and 0.4 mM EDTA. Abl kinase buffer contains 50 mM Tris-HCl (pH 7.5), 10 mM $MgCl_2$, and 0.1 mM EDTA. Fyn buffer contains 25 mM MOPS (pH 7.5), 12.5 mM β-glycerophosphate, 20 mM $MgCl_2$, 25 mM $MnCl_2$, 5 mM EGTA, and 2 mM EDTA.

Preparation of Gold Electrode Surface. The gold electrodes were etched with piranha solution (3:1 H_2SO_4/H_2O_2) for 2 min, and thoroughly washed with Milli-Q water. The electrodes were then hand polished in a series of alumina slurries for 1 min each (1.0, 0.3, and 0.05 μm). The electrodes were electrochemically cleaned using cyclic voltammetry in a solution of 0.5 M KOH at 0.5 V s^{-1} in the −2 to 0 V range. Finally, the electrodes were cleaned using cyclic voltammetry in a solution of 0.5 M H_2SO_4 in the 0−1.5 V range at 0.5 V s^{-1} until a stable gold redox signal was obtained. Electrodes were then rinsed with Milli-Q water followed by ethanol and dried under a gentle stream of nitrogen. The electrodes were then immersed in a 2 mM solution of lipoic acid *N*-succinimide active ester (Lip-NHS) in ethanol for 48 h at 5 °C.

Tau Immobilization. Upon incubation completion, the electrodes were rinsed in ethanol and dried under nitrogen before being rinsed in tau buffer. The electrodes were then immersed into 10 μL of a tau buffer solution (50 mM Tris·HCl pH 7.4, 150 mM NaCl, and 10% glycerol) with 50 μg mL^{-1} tau 410 for 16 h at 5 °C. All electrodes were rinsed in tau buffer and then immersed in a 100 mM solution of ethanolamine in ethanol for 1 h at room temperature to block unreacted active ester. After incubation, the electrodes were rinsed in ethanol and backfilled with a 10 mM solution of hexanethiol in ethanol for 30 min at room temperature. The electrodes were rinsed a final time with ethanol followed by tau buffer prior to kinase reaction. After rinsing with kinase reaction buffer, the electrodes were incubated in a 10 μL reaction mixture containing 1 μg mL^{-1} kinase, 200 mM Fc-ATP, and kinase buffer for 2 h at 37 °C. The electrodes were then rinsed with kinase buffer and water prior to measurement. Sequential kinase reactions were carried out after the electrode was rinsed thoroughly with water and dried under nitrogen. A second mixture containing 1 μg mL^{-1} kinase, 200 mM Fc-ATP, and kinase buffer was placed on the electrode surface and incubated at 37 °C for 2 h. The electrode was rinsed again with kinase assay buffer and water prior to second measurement.

Solution Fc-Phosphorylation. A solution of 50 μg mL^{-1} tau 410, 1 μg mL^{-1} kinase, and 200 mM Fc-ATP was prepared and incubated at 37 °C for 2 h. The mixture was then heated at 94 °C for 4 min to deactivate the kinase. For sequential phosphorylation, 1 μg/mL of a second kinase, 200 mM Fc-ATP, and kinase buffer were added. This solution was incubated again for 2 h at 37 °C and heated for 4 min at 94 °C. A volume of 10 μL of each reaction mixture was then placed on an activated electrode, previously incubated in a 2 mM solution of Lip-NHS for 16 h at 5 °C, to immobilize tau. After rinsing electrodes with the kinase buffer and ethanol, the electrodes were then immersed in a 100 mM solution of ethanolamine for 1 h, followed by incubation in 10 mM hexanethiol for 30 min, at room temperature. The electrodes were then rinsed in ethanol and water then measured.

Electrochemical Measurements. All electrochemical measurements were performed in 2 M sodium perchlorate buffer (pH 6.1) using a three electrode system with Ag/AgCl as reference electrode, Pt wire as auxiliary electrode, and tau-modified gold electrode as working electrode. Cyclic voltammetry was performed at a scan rate of 0.1 V s^{-1} unless otherwise specified, in the 0−0.6 V potential range. Square wave voltammetry was performed in the 0.1−0.6 V potential range at 15 Hz frequency. All electrochemical data reported represent an average of triplicate measurements.

SPR Antibody Assay. SPR analysis was carried out using gold SPR chips purchased from GWC Inc. Gold SPR chips were prepared following the same procedure as reported above for the electrode surface. After blocking and backfilling, the SPR chip was blocked again with LICOR solution (Licor Biosciences) to prevent nonspecific antibody adsorption. Next, SPR chips were rinsed in TBST buffer three times, dried under a gentle stream of nitrogen and fixed to the experimental apparatus. All SPR measurements were recorded on a GWC SPR imager II (GWC Inc. Madison, WI). The SPR pixel intensities were monitored and quantified. The rate constant, k_{on}, values were determined after fitting the rising portion of the experimental SPR curves to the 1:1 binding isotherms (Supporting Information Figures S18−S22).

X-ray Photoelectron Spectroscopy. The samples were analyzed by X-ray photoelectron spectroscopy (XPS) using a Kratos Axis Ultra X-ray photoelectron spectrometer. XPS can detect all elements except hydrogen and helium, probes the surface of the sample to a depth of 7−10 nm, and has detection limits ranging from 0.1 to 0.5 atom % depending on the element. Survey scan analyses were carried out with an analysis area of 300 × 700 μm^2 and a pass energy of 160 eV. High resolution analyses were carried out with an analysis area of 300 × 700 μm^2 and a pass energy of 20 eV.

Time-of-Flight Secondary Ion Mass Spectrometry. The samples were analyzed by using a TOF-SIMS IV instrument (ION-TOF GmbH, Munster, Germany) which was equipped with a Bi liquid metal ion source. The cycle time for the processes of bombardment and detection was 100 μs (or 10 kHz). For all measurements, a 25 keV Bi_3^+ cluster primary ion beam with a pulse width of 12 ns (before bunching) was employed (target current of ∼1 pA). The primary ion pulse width was 2 nA based on the measured peak width of H^+. A pulsed, low energy electron flood was used to neutralize sample charging. For each sample, spectra were collected from 128 × 128 pixels over an area of 500 μm × 500 μm for 60 s. Positive and negative ion spectra were internally calibrated by using H^+, C^+, and CH^+ and H^-, C^-, and CH^- signals, respectively. Mass resolutions of $C_2H_3^+$, $C_3H_5^+$, C_2H^-, and SO_3^- were 3700, 4300, 3100, and 4500, respectively. The Au_3^- peak was at 590.900 m/z, and its position in a spectrum calibrated was 590.843 m/z. Two spots per sample were analyzed using a random approach.

■ ASSOCIATED CONTENT

Ⓢ Supporting Information

Electrochemical data, XPS survey scans and XPS high resolution spectra, TOF-SIMS spectra, and SPR fitting curves. This material is available free of charge via the Internet at http://pubs.acs.org.

■ AUTHOR INFORMATION

Corresponding Author

*E-mail: bernie.kraatz@utoronto.ca.

Author Contributions

All authors have given approval to the final version of the manuscript.

Funding

Funding from NSERC, the University of Toronto is gratefully acknowledged.

Notes

The authors declare no competing financial interest.

■ ABBREVIATIONS

Src, sarcoma-related kinase; Abl, Abelson kinase; GSK-3β, glycogen synthase kinase-3β; CV, cyclic voltammetry; SWV, square-wave voltammetry

■ REFERENCES

(1) Spillantini, M. G., and Goedert, M. (1998) Tau protein pathology in neurodegenerative diseases. *Trends Neurosci. 21*, 428−433.
(2) Lee, V. M.-Y., Goedert, M., and Trojanowski, J. Q. (2001) Neurodegenerative tauopathies. *Annu. Rev. Neurosci. 24*, 1121−1159.
(3) Grundke-Iqbal, I., Iqbal, K., Tung, Y. C., Wisniewski, H. M., and Binder, L. I. (1986) Abnormal phosphorylation of the microtubule-associated protein tau (tau) in Alzheimer cytoskeletal pathology. *Proc. Natl. Acad. Sci. U.S.A. 83*, 4913−4917.
(4) Goedert, M., Wischik, C. M., Crowther, R. A., Walker, J. E., and Klug, A. (1988) Cloning and sequencing of the cDNA encoding a core protein of the paired helical filament of Alzheimer disease: identification as the microtubule-associated protein tau. *Proc. Natl. Acad. Sci. U.S.A. 85*, 4051−4055.
(5) Kondo, J., Honda, T., Mori, H., Hamanda, Y., and Miura, R. (1988) The carboxyl third of tau is tightly bound to paired helical filaments. *Neuron 1*, 827−834.
(6) Lee, V. M.-Y., Balin, B. J., Otvos, L., Jr., and Trojanowski, J. Q. (1991) A68: a major subunit of paired helical filaments and derivatized forms of normal tau. *Science 251*, 675−678.
(7) Manning, G., Whyte, D. B., Martinez, R., Hunter, T., and Sudarsanam, S. (2002) The protein kinase complement of the human genome. *Science 298*, 1912−1934.
(8) Schweers, O., Schonbrunn-Hanebeck, E., Marx, A., and Mandelkow, E. (1994) Structural studies of tau protein and Alzheimer paired helical filaments show no evidence for beta-structure. *J. Biol. Chem. 269*, 24290−24297.
(9) Friedhoff, P., von Bergen, M., Mandelkow, E.-M., Davies, P., and Mandelkow, E. (1998) A nucleated assembly mechanism of Alzheimer paired helical filaments. *Proc. Natl. Acad. Sci. U.S.A. 95*, 15712−15717.
(10) Buee, L., Bussiere, T., Buee-Scherrer, V., Delacourte, A., and Hof, P. R. (2000) Tau protein isoforms, phosphorylation and role in neurodegenerative disorders. *Brain Res. Rev. 33*, 95−130.
(11) Hanger, D. P., Hughes, K., Woodgett, J. R., Brion, J. P., and Anderton, B. H. (1992) Glycogen synthase kinase-3 induced Alzheimer's disease-like phosphorylation of tau: generation of paired helical filament epitopes and neuronal localization of the kinase. *Neurosci. Lett. 147*, 58−62.
(12) Derkinderen, P., Scales, T. M. E., Hanger, D. P., Leung, K. Y., Byers, H. L., Ward, M. A., Lenz, C., Price, C., Bird, I. N., Perera, T., Kellie, S., Williamson, R., Noble, W., van Etten, R. A., Leroy, K., Brion, J. P., Reynolds, C. H., and Anderton, B. H. (2005) Tyrosine 394 is phosphorylated in Alzheimer's paired helical filament tau and in fetal tau with c-Abl as the candidate tyrosine kinase. *J. Neurosci. 25*, 6584−6593.
(13) Lee, G. (2005) Tau and src family tyrosine kinases. *Biochim. Biophys. Acta 1739*, 323−330.
(14) Lee, G., Thangavel, R., Sharma, V. M., Litersky, J. M., Bhaskar, K., Fang, S. M., Do, L. H., Andreadis, A., Van Hoesen, G., and Ksiezak-Reding, H. (2004) Phosphorylation of tau by fyn: implications for Alzheimer's disease. *J. Neurosci. 24*, 2304−2312.
(15) Moore, K. J., El Khoury, J., Medeiros, L. A., Terada, K., Geula, C., Luster, A. D., and Freeman, M. W. (2002) A CD36-initiated signaling cascade mediates inflammatory effects of beta-amyloid. *J. Biol. Chem. 277*, 47373−47379.
(16) Lambert, M. P., Barlow, A. K., Chromy, B. A., Edwards, C., Freed, R., Liosatos, M., Morgan, T. E., Rozovsky, I., Trommer, B., Viola, K. L., Wals, P., Zhang, C., Finch, C. E., Krafft, G. A., and Klein, W. L. (1998) Diffusible, nonfibrillar ligands derived from Abeta1−42 are potent central nervous system neurotoxins. *Proc. Natl. Acad. Sci. U.S.A. 95*, 6448−6453.
(17) Tatebayashi, Y., Haque, N., Tung, Y. C., Iqbal, K., and Grundke-Iqbal, I. (2004) Role of tau phosphorylation by glycogen synthase kinase-3β in the regulation of organelle transport. *J. Cell Sci. 117*, 1653−1663.
(18) Lund, E. T., McKenna, R., Evans, D. B., Sharma, S. K., and Mathews, W. R. (2001) Characterization of the in vitro phosphorylation of human tau by tau protein kinase II (cdk5/p20) using mass spectrometry. *J. Neurochem. 76*, 1221−1232.

(19) Barghorn, S., and Madelkow, E. (2002) Toward a unified scheme for the aggregation of tau into Alzheimer paired helical filaments. *Biochemistry 41*, 14885−14896.
(20) Friedhoff, P., Schneider, A., Madelkow, E. M., and Mandelkow, E. (1998) Rapid assembly of Alzheimer-like paired helical filaments from microtubule-associated protein tau monitored by fluorescence in solution. *Biochemistry 37*, 10223−10230.
(21) Schweers, O., Schonbrunn-Hanebeck, E., Marx, A., and Madelkow, E. (1994) Structural studies of the tau protein and Alzheimer paired helical filaments show no evidence for beta-structure. *J. Biol. Chem. 269*, 24290−24297.
(22) Martic, S., Labib, M., Freeman, D., and Kraatz, H.-B. (2011) Probing the role of the linker in ferrocne-ATP conjugates: monitoring protein kinase catalyzed phosphorylations electrochemically. *Chem.—Eur. J. 17*, 6744−6752.
(23) Martic, S., Gabriel, M., Turowec, J. P., and Litchfield, D. W. (2012) Versatile strategy for biochemical, electrochemical and immonoarray detection of protein phosphorylations. *J. Am. Chem. Soc. 134*, 17036−17045.
(24) Martic, S., Beheshti, S., Rains, M. K., and Kraatz, H.-B. (2012) Electrochemical investigations into tau protein phosphorylations. *Analyst 137*, 2042−2046.
(25) Kerman, K., Song, H., Duncan, J. S., Litchfield, D. W., and Kraatz, H.-B. (2008) Peptide biosensor for the electrochemical measurements of protein kinase activity. *Anal. Chem. 80*, 9395−9401.
(26) Johnson, S. A., and Hunter, T. (2005) Kinomics: methods for deciphering the kinome. *Nat. Methods 2*, 17−25.
(27) Sloboda, R. D., Rudolph, S. A., Rosenbaum, J. L., and Greengard, P. (1975) Cyclic AMP-dependent endogenous phosphorylation of a microtubule-associated protein. *Proc. Natl. Acad. Sci. U.S.A. 72*, 177−181.
(28) Nakanishi, K., Sakiyama, T., Kumada, Y., Imamura, K., and Imanaka, H. (2008) Recent advances in controlled immobilization of proteins onto the surface of the solid substrate and its possible application to proteomics. *Curr. Proteomics 5*, 161−175.
(29) Shimizu, M., Kobayashi, K., Morii, H., Mitsui, K., Knoll, W., and Nagamune, T. (2003) Secondary structure analyses of protein films on gold surfaces by circular dichroism. *Biochem. Biophys. Res. Commun. 310*, 606−611.
(30) Hollander, Z., and Katchalski-Katzir, E. (1998) Use of monoclonal antibodies to detect conformational alterations in lactate dehydrogenase isoenzyme 5 on heat denaturation and on adsorption to polystyrene plates. *Mol. Immunol. 23*, 927−933.
(31) Nakanishi, K., Sakiyama, T., and Imamura, K. (2001) On adsorption of proteins on soldi surfaces, a common but very complicated pehnomenon. *J. Biosci. Bioeng. 91*, 233−244.
(32) Norde, W., and Zoungrana, T. (1998) Surface-induced changes in the structure and activity of enzymes physically immobilized at solid-liquid interface. *Biotechnol. Appl. Biochem. 28*, 133−143.
(33) Johnson, B. N., and Mutharasan, R. (2012) pH effect on protein G orientation on gold surfaces and characterization of adsorption thermodynamics. *Langmuir 28*, 6928−6934.
(34) Wagner, M. S., and Castner, D. G. (2001) Characterization of adsorbed protein films by time-of-flight secondary ion mass spectrometry with principal component analysis. *Langmuir 17*, 4649−4660.
(35) Wang, H., Castner, D. G., Ratner, B. D., and Jiang, S. (2004) Probing the orientation of surface-immobilized immunoglobulin G by time-of-flight secondary ion mass spectrometry. *Langmuir 20*, 1877−1887.
(36) Lhoest, J. B., Detrait, E., van den Bosch de Aguilar, P., and Bertrand, P. (1998) Fibronectin absorption, conformation, and orientation on polystyrene substrates studied by radiolabeling, XPS, and TOF-SIMS. *J. Biomed. Mater. Res. 41*, 95−103.
(37) Tidwell, C. D., Castner, D. G., Golledge, S. L., Ratner, B. D., Meyer, K., Hagenhoff, B., and Benninghoven, A. (2001) Static time-of-flight secondary ion mass spectrometry and X-ray photoelectron spectroscopy characterization of adsorbed albumin and fibronectin films. *Surf. Interface Anal. 31*, 724−733.
(38) Martic, S., Labib, M., and Kraatz, H.-B. (2011) Enzymatically modified peptide surfaces: towards general electrochemical sensor platform for protein kinase catalyzed phosphorylations. *Analyst 136*, 107−112.
(39) Xia, N., May, C. J., McArthur, S. L., and Castner, D. G. (2002) Time-of-flight secondary ion mass spectrometry analysis of conformational changes in adsorbed protein films. *Langmuir 18*, 4090−4097.
(40) Nuzzo, R. G., Zegarski, B. R., and Dubois, L. H. (1987) Fundamental studies of the chemisorption of organosulfur compounds on gold (111). Implications for molecular self-assembly on gold surfaces. *J. Am. Chem. Soc. 109*, 733−740.
(41) (a) Castner, D. G., Hinds, K., and Grainger, D. W. (1996) X-ray photoelectron-spectroscopy sulfur 2P study of organic thiol and disulfide binding interactions with gold surfaces. *Langmuir 12*, 5083−5086. (b) Bain, C. D., Biebuyck, H. A., and Whitesides, G. M. (1989) Comparison of self-assembled monolayers on gold: coadsorption of thiols and disulfides. *Langmuir 5*, 723−727.
(42) Ray, S., and Shard, A. G. (2011) Quantitative analysis of adsorbed proteins by X-ray photoelectron spectroscopy. *Anal. Chem. 83*, 8659−8666.
(43) Baio, J. E., Weidner, T., Baugh, L., Gamble, L. J., Stayton, P. S., and Castner, D. G. (2012) Probing the orientation of electrostatically immobilized protein G B1 by time-of-flight secondary ion spectrometry, sum frequency generation, and near-edge X-ray adsorption fine structure spectroscopy. *Langmuir 28*, 2107−2112.
(44) Song, H., Kerman, K., and Kraatz, H.-B. (2008) Electrochemical detection of kinase-catalyzed phosphorylation using ferrocene-conjugated ATP. *Chem. Commun.*, 502−504.